BMB Reports - Manuscript Submission

Manuscript Draft

Manuscript Number: BMB-18-282

Title: Endothelial dysfunction induces atherosclerosis: increased aggrecan expression promotes apoptosis in vascular smooth muscle cells

Article Type: Article

Keywords: Endothelial nitric oxide synthase; Aggrecan; Atherosclerosis; Apoptosis; Vascular smooth muscle cells

Corresponding Author: Eun-Ju Chang

Authors: Sang-Min Kim[1,4,#], Jae-Wan Huh[2,#], Eun-Young Kim[1,3], Min-Kyung Shin[1,3], Ji-Eun Park[1,3], Seong Who Kim[2,3], Bongkun Choi[1,3], Wooseong Lee[2], Bongkun Choi[1,3], Eun-Ju Chang[1,2,3,*]

Institution: [1]Department of Biomedical Sciences and [2]Department of Biochemistry and Molecular Biology and [3]Stem Cell Immunomodulation Research Center, University of Ulsan College of Medicine, [4]Department of Pathology, Yonsei University College of Medicine,

Endothelial dysfunction induces atherosclerosis: increased aggrecan expression promotes apoptosis in vascular smooth muscle cells

Running title: Aggrecan induces apoptosis in VSMCs

Sang-Min Kim [a, d #], *Jae-Wan Huh* [b, #], *Eun-Young Kim* [a, c], *Min-Kyung Shin* [a, c], *Ji-Eun Park* [a, c], *Seong Who Kim* [b, c], *Wooseong Lee* [b], *Bongkun Choi* [a, c, *] & *Eun-Ju Chang* [a, b, c, *]

[a] Department of Biomedical Sciences, Asan Medical Center, University of Ulsan College of Medicine, Seoul 05505, Korea

[b] Department of Biochemistry and Molecular Biology, Asan Medical Center, University of Ulsan College of Medicine, Seoul 05505, Korea

[c] Stem Cell Immunomodulation Research Center, Asan Medical Center, University of Ulsan College of Medicine, Seoul 05505, Korea

[d] Department of Pathology, Yonsei University College of Medicine, Seoul 03722 Korea

Keywords: Endothelial nitric oxide synthase, Aggrecan, Atherosclerosis, Apoptosis, Vascular smooth muscle cells

# These authors are equally contributed.

* Corresponding author.

Eun-Ju Chang: Tel: +82-2-3010-4262; Fax: +82-2-3010-5307; E-mail: ejchang@amc.seoul.kr

Bongkun Choi: Tel: +82-2-3010-4662; Fax: +82-2-3010-5307; E-mail: bkchoi89@hanmail.net

ABSTRACT

Endothelial dysfunction-induced lipid retention is an early feature of atherosclerotic lesion formation. Apoptosis of vascular smooth muscle cells (VSMCs) is one of the major modulating factors of atherogenesis, which accelerates atherosclerosis progression by causing plaque destabilization and rupture. However, the mechanism underlying VSMC apoptosis mediated by endothelial dysfunction in relation to atherosclerosis remains elusive. In this study, we reveal differential expression of several genes related to lipid retention and apoptosis, in conjunction with atherosclerosis, by utilizing a genetic mouse model of endothelial nitric oxide synthase (eNOS) deficiency manifesting endothelial dysfunction. Moreover, eNOS deficiency led to the enhanced susceptibility against pro-apoptotic insult in VSMCs. In particular, the expression of aggrecan, a major proteoglycan, was elevated in aortic tissue of eNOS deficient mice compared to wild type mice, and administration of aggrecan induced apoptosis in VSMCs. This suggests that eNOS deficiency may elevate aggrecan expression, which promotes apoptosis in VSMC, thereby contributing to atherosclerosis progression. These results may facilitate the development of novel approaches for improving the diagnosis or treatment of atherosclerosis.

INTRODUCTION

Endothelial dysfunction is a pathophysiological condition characterized by diminished production of vasodilating factors, mainly nitric oxide (NO), and an increase in endothelium-derived vasoconstrictors (1). NO produced by endothelial nitric oxide synthase (eNOS) in endothelial cells (ECs) plays an important role in proper endothelium functions by regulating vascular homeostasis and the functional endothelium, and acts as an anti-thrombotic and anti-inflammatory barrier for the vascular wall (1). The maintenance of endothelium function is, thus, critical for the protection of the cardiovascular system against atherosclerosis (2-4), myocardial ischemia (5), and unstable angina (6). In this context, endothelium dysfunction is known to be an early feature of atherosclerotic lesion formation and progression (7).

Atherosclerosis is a representative disease, showing progressive and chronic inflammatory pathology of the arterial intima, and it is the leading cause of death in developed countries (8). Progression of this disease is characterized by real-life clinical events of the rupture and thrombosis of atherosclerotic plaques that consist of macrophages, ECs, vascular smooth muscle cells (VSMCs), and different collagen types (8, 9). In the case of vessel damage, VSMCs change from the contractile into the proliferative type, to repair the vascular wall. However, in atherosclerosis, VSMCs become aberrantly regulated and this promotes extracellular matrix formation in plaque areas (10-12). The major atherogenic factors are known to be lipid dysfunction, cell death, arterial lipid accumulation, and inflammatory responses in directing the initiation and development of a prominent feature of advanced atherosclerotic lesion (10, 13, 14). In particular, apoptosis of VSMCs may cause plaque destabilization and rupture by inducing loss of collagen and matrix, accumulation of cell debris, and intimal inflammation, thereby reinforcing atherosclerosis progression (10). This is because the tensile strength of the protective cap mainly depends on structural properties determined by the number of VSMCs and the collagen which they produce (15). VSMC apoptosis may also promote calcification, become procoagulant both locally and systemically, and provoke inflammation (16), further accelerating atherosclerosis progression in later stage. However, the mechanism underlying eNOS

deficiency-mediated induction of VSMC apoptosis in relation to atherosclerosis remains elusive.

In this study, we aimed to investigate the differential gene expression profiles associated with atherosclerosis in aortic tissues using a genetic model of eNOS deficiency, and identify differentially expressed genes related to the pathogenesis of atherosclerosis. We found that eNOS deficiency led to an increase in aggrecan expression, which promotes apoptosis in VSMCs, indicating that NO-deficiency-mediated apoptosis of VSMCs may be involved in the pathological pathways of atherosclerosis. Understanding the changes in gene expression induced by eNOS deficiency could reveal molecular mechanism in atherosclerosis and facilitate the development of novel approaches for improving the diagnosis or treatment of the disease.

RESULTS

Genetic deletion of eNOS increases apoptosis by altering apoptosis-related gene expression in murine aortic tissue

Although previous studies report that eNOS protects against atherosclerosis while eNOS deficiency leads to increased atherosclerosis in a mouse model (4, 17), gene expression changes associated with atherosclerosis in *eNOS*$^{-/-}$ mice have not been investigated. Therefore, we performed Affymetrix Gene-Chip microarray gene expression profiling of aortic tissue isolated from WT and *eNOS*$^{-/-}$ mice to analyze differentially expressed genes in eNOS deficient mouse manifesting endothelial dysfunction. We found that the expression of genes related to the pathogenesis of atherosclerosis was elevated in *eNOS*$^{-/-}$ mice. These genes include *fibronectin 1* (*FN1*; response to stress, adhesion and extracellular molecules (ECM)), *connective tissue growth factor* (*CTGF*; adhesion, ECM and cell growth), and *thrombospondin 4* (*THBS4*; adhesion and ECM) (Supplementary Table 1).

Evidence suggests that apoptosis in atherosclerotic lesions is responsible for prominent atherogenesis (10, 13, 14). Therefore, we then examined differential apoptosis-related gene expression profiles of WT and *eNOS*$^{-/-}$ mice, and found that the expressions of *Tnfrsf11b* (tumor necrosis factor receptor superfamily, member 11b) and *Dapk1* (death associated protein kinase 1) were dysregulated in the *eNOS*$^{-/-}$ aorta (Supplementary Table 1). In order to verify the microarray results, we performed qPCR for *Tnfrsf11b* and *Dapk1* using total RNA extracted from WT and *eNOS*$^{-/-}$ aortas. Being consistent with microarray expression profiling data, these genes were found to be upregulated in the *eNOS*$^{-/-}$ aorta compared with those of WT (Fig. 1C).

We next evaluated apoptosis in aortic tissue isolated from WT and *eNOS*$^{-/-}$ mice. TUNEL assay revealed that *eNOS*$^{-/-}$ mice aortic tissue is sensitized to undergo apoptosis compared to that of WT, as shown by increased TUNEL-positive cells which co-stained against α-SMA, the representative marker of VSMC (Fig. 1A and 1B).

Increased apoptosis in eNOS$^{-/-}$ VSMCs

Cell death is an important factor for plaque rupture in atherosclerosis (10, 13). In particular, VSMC apoptosis in atherosclerotic plaque could be detrimental to plaque stability and increase the risk for thrombosis (10, 14). We observed an increased rate of apoptosis in aortic tissue from *eNOS*$^{-/-}$ mouse (Fig. 1) and thus investigated whether eNOS deficiency leads to induction of apoptosis in VSMC utilizing TUNEL assay. While WT VSMC showed negligible evidence of apoptosis, *eNOS*$^{-/-}$ VSMC showed presence of apoptosis as indicated by TUNEL positive staining (Fig. 2A). Followed by serum deprivation, apoptosis was further increased in *eNOS*$^{-/-}$ VSMC, as shown by increased TUNEL positive staining (Fig. 2A and 2B). To confirm eNOS deficiency-induced apoptosis, VSMCs were also subjected to Annexin V/PI staining and analyzed by flow cytometry. We observed enhanced apoptosis in *eNOS*$^{-/-}$ VSMC, as shown by 14.9% annexin V positive cells, whereas it was only 3.4% in WT VSMCs (Fig. 2C). *eNOS*$^{-/-}$ VSMC exhibited a marked increase (4.4 fold; $p < 0.05$) compared with WT VSMCs in the apoptotic cell fraction assessed by FACs analysis of an annexin V staining assay (Fig. 2D), suggesting that VSMC apoptosis was promoted by eNOS deficiency.

eNOS deficiency leads to elevated expression of aggrecan which induces apoptosis in VSMCs

Previous reports showed that deposition of proteoglycan is selectively enhanced in the intima of advanced atherosclerotic lesions (18, 19), and aggrecan induces apoptosis in chondrocytes and murine thymoma cells (20, 21). Thus, we next determined whether eNOS deficiency leads to accumulation of aggrecan in aortic tissue and, in turn, aggrecan induces apoptosis in VSMC. The major lipoprotein-binding proteoglycans, *aggrecan* (*Acan*), *biglycan* (*Bgn*), and *versican* (*Vcan*) showed higher mRNA expressions in *eNOS*$^{-/-}$ mice compared to those of WT in microarray expression profiling data (Fig. 3A and 3B). In particular, aggrecan mRNA expression was significantly higher in *eNOS*$^{-/-}$ mice and these results were confirmed using qPCR (Fig. 3B). Aggrecan protein expression was higher in aortic sinus tissue from eNOS deficient mouse compared with that of WT mouse, as evidenced by immunoblot assay (Fig. 3C) and increased aggrecan positive staining (Fig. 3D).

Enhanced apoptosis by aggrecan and NO-mediated aggrecan gene expression in *eNOS*$^{-/-}$ VSMCs

The administration of aggrecan induced apoptosis was modest, at a concentration of 1 μg/ml in the presence of serum, whereas upon serum withdrawal aggrecan promoted VSMC apoptosis in a dose-dependent manner, as shown by TUNEL staining (Fig. 4A). Annexin V/PI staining also revealed the dose-dependent increase in apoptosis in response to aggrecan treatment in these cells (Fig. 4B). Treatment of VSMC with DETA-NO, a NO donor, induced a dose-dependent decrease of gene expression of aggrecan (Fig. 4C). In contrast, L-NAME, an NOS inhibitor, increased aggrecan mRNA in a dose-dependent manner (Fig. 4D). Moreover, DETA-NO treatment decreased the number of apoptotic VSMCs (Fig. 4E). Altogether, these results suggest that eNOS deficiency may induce expression of aggrecan, which in turn promotes apoptosis in VSMC, thereby triggering atherosclerosis.

DISCUSSION

To investigate the contribution of endothelial dysfunction in pathological conditions of atherosclerosis, we used a genetic model of eNOS deficiency and showed that several genes associated with lipid retention and apoptosis, implicated in the pathogenesis of atherosclerosis, were differentially expressed in *eNOS*$^{-/-}$ mouse (Fig. 1), demonstrating the involvement of endothelium dysfunction in pathological pathways deriving atherosclerosis.

In atherosclerotic aorta of apoE-KO mouse, the expression level of a disintegrin and metalloprotease with thrombospondin motifs-5 (ADAMTS-5) was markedly reduced, which cleaves aggrecan, one of the major lipoprotein-binding proteoglycans (22). Such results raise the possibility that aggrecan may be accumulated in atherosclerotic plaques. Indeed, we found that aortic sinus tissue from eNOS deficient mice possessing atherosclerotic regions expressed higher amounts of aggrecan than WT mice (Fig. 3). In line with this result, selective deposition of proteoglycan such as aggrecan, biglycan, and veriscan was enhanced in the intima of advanced atherosclerotic lesions (18, 19) and apolipoprotein B-containing lipoproteins are trapped by these proteoglycans, initiating atherosclerosis in the arterial intima through macrophage accumulation and lipid core formation (22).

It has been reported that aggrecan induces apoptosis in chondrocytes (20) and murine thymoma cell line expressing human Fas (21). As VSMC apoptosis may cause plaque destabilization and rupture, accelerating atherosclerosis progression (10, 15), we determined whether aggrecan affects apoptosis in VSMC. We found aggrecan-mediated induction of apoptosis in VSMC (Fig. 4) for the first time as far as we know. This result suggests that VSMC apoptosis mediated by elevated aggrecan may be associated with atherosclerosis progression in eNOS deficient mice. In this context, Stevens et al. reported that NO enhances aggrecan degradation by inducing aggrecanase activity at posttranscriptional level (23), suggesting that NO deficiency is likely to induce accumulation of aggrecan protein. Nonetheless, we found that eNOS deficiency increases expression of aggrecan mRNA as evidenced by microarray data profiling and qPCR, as well as aggrecan protein as shown by IHC in animal model (Fig. 3). Taken together, these results suggest that eNOS deficiency may induce

elevated expression of aggrecan which promotes apoptosis in VSMC, thereby triggering atherosclerosis.

We revealed several unrecognized genes potentially implicated in the pathogenesis of apoptosis and lipid retention, as well as atherosclerosis, by utilizing a genetic model of eNOS deficiency. We showed that eNOS deficiency may induce elevated expression of aggrecan in VSMCs, which promotes apoptosis and subsequent progression of atherosclerosis. This suggests that amplified VSMC apoptosis mediated by elevated level of aggrecan may be involved in pathological pathways of atherosclerosis due to endothelial dysfunction. These results may shed light on the mechanisms by which endothelium dysfunction contributes to the progression of atherosclerosis. Future research unraveling the regulation of aggrecan-mediated apoptosis in the cardiovascular system could provide new therapeutic avenues for prevention or control of atherosclerosis.

MATERIALS AND METHODS

Materials

Bafilomycin A1 and monoclonal anti-β-actin antibody (Ab) were purchased from Sigma–Aldrich (St Louis, MO, USA). Recombinant aggrecan was obtained from R and D (Minneapolis, MN, USA). Self-quenched BIODIPY dye conjugates of bovine serum albumin (DQ-BSA) and DAPI (4′′, 6-diamidino-2-phenylindole) were obtained from Invitrogen (Carlsbad, CA, USA). Donkey FITC-conjugated anti-mouse IgG was purchased from Jackson Immunoresearch (West Grove, PA, USA). Anti-aggrecan polyclonal antibody was purchased from Abcam (Cambridge, MA, USA).

Cells culture and animals

eNOS$^{-/-}$ mice were purchased from Jackson laboratories (Bar Harbor, ME, USA). All animal experiments were performed according to protocols approved by the Institutional Committee for Use and Care of Laboratory animals. The studies with mice were conducted according to the protocol granted by the Ethics Committee of Ulsan University (Seoul, Korea,) and conformed to the Guide for the Care and Use of Laboratory Animals published by NIH. The application form included a statement guaranteeing strict observation to the animal's rights. Female mice were maintained in a pathogen free facility with 12 hr light/dark cycle. Murine VSMCs were isolated from the aorta by enzyme isolation and maintained in Dulbecco modified eagle medium (DMEM, Hyclone, South Logan, UT, USA) supplemented with 10% fetal bovine serum (Hyclone), penicillin (100 U·ml^{-1}, Life Technologies, Carlsbad, CA, USA), and streptomycin sulfate (Life Technologies) (24).

Immunofluorescence staining and confocal microscopy

The animals were anesthetized and perfused with PBS, pH 7.4. The hearts were dissected, embedded in OCT compound (Sakura Finetek, Torrance, CA, USA), and snap-frozen in liquid nitrogen. Serial 5 μm sections were taken through the aortic sinus. Immunohistochemistry (IHC) was carried out

utilizing the EnVision™ G|2 Doublestain System and rabbit/mouse (DAB+/Permanent Red) in accordance to the manufacturer's protocol (Dako, Carpinteria, CA, USA). Sections were fixed with paraformaldehyde and then permeabilized with 0.25% Triton X-100 in PBS. After being blocked with dual endogenous enzyme-blocking reagent, sections were incubated with primary antibody against aggrecan for 30 minutes at RT, and the polymer/HRP system was applied for detection. Corresponding rabbit sera were used as negative controls. Sections were stained with 4′,6-diamidino-2-phenylindole (DAPI) and α-smooth muscle actin (α-SMA). Terminal deoxynucleotidyl transferase-mediated dUTP-biotin nick-end-labeling (TUNEL) staining for apoptotic nuclei was performed using In Situ Cell Death Detection Kit (Roche, Germany) in accordance to the manufacturer's instructions. Digital images were acquired using a confocal laser-scanning microscope (LSM 710, Carl Zeiss).

RNA isolation

Total RNA was extracted from the aorta of WT and *eNOS*$^{-/-}$ mice using RNeasy Lipid Tissue Kit (QIAGEN, Hilden, Germany). RNA quality was assessed by Agilent 2100 bioanalyzer using the RNA 6000 Nano Chip (Agilent Technologies, Amstelveen, Netherlands), and its quantity was determined by ND-1000 Spectrophotometer (NanoDrop Technologies, Inc., Wilmington, DE, USA).

Gene Expression Profiling (Microarray)

Global gene expression analyses of aorta specimens from WT and *eNOS*$^{-/-}$ mice were performed using Affymetrix GeneChip® Mouse Gene 2.0 ST Array (Affymetrix, Santa Clara, CA, USA). Sample preparation was performed according to the instructions and recommendations provided by the manufacturer. In brief, 300 ng of total RNA from each sample was converted to double-strand cDNA using a random hexamer incorporating a T7 promoter. Amplified RNA was generated from the double-stranded cDNA template through an *in vitro* transcription reaction and purified with the Affymetrix sample cleanup module. cDNA was regenerated through random-primed reverse transcription using a dNTP mix which contained dUTP. The cDNA was then fragmented by UDG and

APE 1 restriction endonucleases, and end-labeled by terminal transferase reaction incorporating a biotinylated dideoxynucleotide. Fragmented end-labeled cDNA was hybridized to the GeneChip® Mouse Gene 2.0 ST arrays for 17 hr at 45 °C as described in the Gene Chip Whole Transcript Sense Target Labeling Assay Manual (Affymetrix). After hybridization, the chips were stained, washed in a Genechip Fluidics Station 450 (Affymetrix) and scanned using a Genechip Array scanner 3000 7G (Affymetrix) (25).

Data processing and analysis

The intensity values of CEL files were normalized to remove bias between the samples, using the Robust Multi-Average algorithm implemented in the Affymetrix Expression Console software version 1.3.1. The normalized data were imported into the statistical programming environment R (Version3.0.2) for further analysis, such as density and MA plots with tools available from the Bioconductor Project (http://www.bioconductor.org). In order to classify the co-expression gene groups which have similar expression patterns, hierarchical clustering analysis was performed with the Multi Experiment Viewer software version 4.4 (http://www.tm4.org). The web-based tool Database for Annotation, Visualization, and Integrated Discovery was used to perform the biological interpretation of the differentially expressed genes. Genes were classified based on the information of the gene function in Gene ontology and KEGG pathway databases. (http://david.abcc.ncifcrf.gov/home.jsp) The complete data set is available with NCBI GEO accession number GSE123855.

Quantitative real-time PCR (qPCR)

Quantitative real-time PCR was performed to validate the microarray experiment with the same RNA used on the microarray, using a Power SYBR Green 1-Step Kit and the ABI 7000 Real Time PCR System (Applied Biosystems, Carlsbad, CA, USA) following manufacturer's instructions. Gene expression was normalized to *GAPDH* gene and the quantity of target gene was calculated according to the comparative C_T method.

Western blot assay

Cells were lysed, and protein lysates were resolved on sodium dodecyl sulfate–polyacrylamide gel electrophoresis (SDS-PAGE) and electophoretically transferred to a polyvinyli-dene difluoride membrane (Bio-Rad, Hercules, CA, USA). Nonspecific interactions were blocked using 5% BSA solution in Tris–buffered saline (20 mM Tris/HCl, pH 7.6, 150 mM NaCl, and 0.1% Triton X-100) for 1 hr and membranes were then incubated with the indicated primary antibodies overnight at 4 °C. Membranes were incubated with the appropriate secondary antibodies conjugated with horseradish peroxidase and immunoreactivity was detected by the use of an enhanced chemiluminescence detection kit (Millipore, Billerica, MA, USA).

TUNEL assay

Apoptosis of VSMCs from WT and *eNOS*$^{-/-}$ mice were induced with serum deprivation. VSMC was also treated with various concentrations of aggrecan in the presence or absence of serum and TUNEL staining for apoptotic nuclei was performed.

Annexin V/ propidium iodide (PI) staining

Apoptosis was detected by annexin-V and propidium iodide (PI) staining using the FITC Annexin-V Apoptosis Detection Kit I (BD Pharmingen, San Diego, CA, USA). Briefly, VSMCs were washed twice in cold PBS, and resuspended in 1× Annexin-V binding buffer (10 mM HEPES/NaOH, pH 7.4; 140 mM NaCl; 2.5 mM $CaCl_2$). Cells were then stained with Annexin-V-FITC and PI, and incubated for 15 minutes at 4°C in the dark and analyzed with a FACScalibur flow cytometer and analyzed in CellQuest software.

Statistical analysis

All quantitative experiments were performed at least in triplicate and the data values are presented as

the mean ± standard deviation. Mann-Whitney test (Fig. 1B and Fig. 2D) or Kruskal-Wallis test (Fig. 1C, Fig. 2B, Fig. 3B and Fig. 4) were used to determine significance. *p* value of less than 0.05 was considered statistically significant.

ACKNOWLEDGMENTS

This work was supported by the National Research Foundation of Korea (NRF) MRC grant (2018R1A5A2020732) funded by the Korean government (MSIT).

CONFLICTS OF INTEREST

All authors declare no conflicts of interest.

FIGURE LEGENDS

Fig. 1. Increased apoptosis in the aortic sinus from *eNOS*$^{-/-}$ mice. (A) Representative images of α-SMA (stained in red) and TUNEL staining showing apoptotic cells (stained in green) in the aortic sinus from WT and *eNOS*$^{-/-}$ mice. Scale bars, 20 μm. (B) The number of TUNEL-positive cells in the aortic sinus of WT and *eNOS*$^{-/-}$ mice (mean ± SD). *$p < 0.05$ compared to WT control. (C) Validation of microarray experiment by quantitative real-time PCR for apoptosis-related genes including *TNFRSF11B* and *DAPK1* in *eNOS*$^{-/-}$ relative to WT controls. *$p < 0.05$ and **$p < 0.005$ compared to WT control. *p* values were calculated using Mann-Whitney test (Fig. B) or Kruskal-Wallis test (Fig. C).

Fig. 2. Enhanced apoptosis in *eNOS*$^{-/-}$ vascular smooth muscle cells (VSMCs). (A) Representative light microscopy (upper panels) and images of TUNEL staining (lower panels) showing apoptotic cells (stained in green) in VSMCs from WT and *eNOS*$^{-/-}$ mice in the presence or absence of serum deprivation. Scale bar, 100 μm. (B) The percentage of apoptosis was calculated as percent of TUNEL-positive cells out of total cells (mean ± SD). NS, not significant; *$p < 0.05$ compared to WT VSMC incubated without serum. (C) Flow cytometry analysis of annexin-V and propidium iodide (PI) staining of apoptotic cells in VSMCs from WT and *eNOS*$^{-/-}$ mice. (D) Quantification of annexin-V positive apoptotic cells (annexin-V positive and PI negative + annexin-V and PI double positive cells). *$p < 0.05$ compared to WT VSMC. *p* values were calculated using Kruskal-Wallis test (Fig. B) or Mann-Whitney test (Fig. D).

Fig. 3. Elevated expression of aggrecan in aorta from *eNOS*$^{-/-}$ mouse. (A) Gene expression profiles of remodeling-associated genes. Transcripts that are upregulated and downregulated are shown in red and green, respectively. The columns represent the aorta samples from WT or *eNOS*$^{-/-}$ mice. (B) The levels of mRNA expression of *aggrecan* (*Acan*), *biglycan* (*Bgn*), and *versican* (*Vcan*) were compared

in aorta from WT and *eNOS*$^{-/-}$ mice using qPCR. *$p < 0.05$ compared to WT control. p values were calculated using Kruskal-Wallis test. (C) Protein expression of aggrecan and β-actin were detected by western blotting in VSMCs. (D) Representative photographs of immunohistochemistry staining of aggrecan in aortic sinus sections from WT and *eNOS*$^{-/-}$ mice. Scale bar, 100 μm.

Fig. 4. Induction of apoptosis by aggrecan and NO-mediated gene expression of aggrecan in *eNOS*$^{-/-}$ VSMCs. (A) VSMCs from WT and *eNOS*$^{-/-}$ mice were treated with various concentrations of aggrecan, followed by induction of apoptosis with serum deprivation. The percentage of TUNEL-positive cells was determined using TUNEL staining. (B) Quantification of annexin-V positive apoptotic cells in VSMC treated with indicated concentrations of aggrecan. *$p < 0.05$ and **$p < 0.005$ compared to vehicle control. (C, D) VSMCs were treated with the indicated concentrations of DETA-NO (C) or L-NAME (D) and relative gene expression of ACAN was quantitated using qPCR. GAPDH was used as an internal control (mean ± SD). (E) VSMCs were treated with DETA-NO, followed by induction of apoptosis with serum deprivation. The percentage of TUNEL-positive cells was determined using TUNEL staining. *$p < 0.05$ and **$p < 0.005$ compared to vehicle control. p values were calculated using Kruskal-Wallis test.

REFERENCES

1. Furchgott RF and Zawadzki JV (1980) The obligatory role of endothelial cells in the relaxation of arterial smooth muscle by acetylcholine. Nature 288, 373-376
2. Davignon J and Ganz P (2004) Role of endothelial dysfunction in atherosclerosis. Circulation 109, III27-32
3. Mooradian DL, Hutsell TC and Keefer LK (1995) Nitric oxide (NO) donor molecules: effect of NO release rate on vascular smooth muscle cell proliferation in vitro. J Cardiovasc Pharmacol 25, 674-678
4. Ponnuswamy P, Schröttle A, Ostermeier E et al (2012) eNOS protects from atherosclerosis despite relevant superoxide production by the enzyme in apoE mice. PLoS One 7, e30193
5. Flammer AJ, Anderson T, Celermajer DS et al (2012) The assessment of endothelial function: from research into clinical practice. Circulation 126, 753-767
6. Bogaty P, Hackett D, Davies G and Maseri A (1994) Vasoreactivity of the culprit lesion in unstable angina. Circulation 90, 5-11
7. Cooke JP, Singer AH, Tsao P, Zera P, Rowan RA and Billingham ME (1992) Antiatherogenic effects of L-arginine in the hypercholesterolemic rabbit. J Clin Invest 90, 1168-1172
8. Lusis AJ (2000) Atherosclerosis. Nature 407, 233-241
9. Libby P, Ridker PM and Hansson GK (2011) Progress and challenges in translating the biology of atherosclerosis. Nature 473, 317-325
10. Clarke MC, Figg N, Maguire JJ et al (2006) Apoptosis of vascular smooth muscle cells induces features of plaque vulnerability in atherosclerosis. Nat Med 12, 1075-1080
11. Klouche M, Peri G, Knabbe C et al (2004) Modified atherogenic lipoproteins induce expression of pentraxin-3 by human vascular smooth muscle cells. Atherosclerosis 175, 221-228
12. Zhang MJ, Zhou Y, Chen L et al (2016) Impaired SIRT1 promotes the migration of vascular smooth muscle cell-derived foam cells. Histochem Cell Biol 146, 33-43
13. Kockx MM and Herman AG (2000) Apoptosis in atherosclerosis: beneficial or detrimental? Cardiovasc Res 45, 736-746
14. Martinet W and Kockx MM (2001) Apoptosis in atherosclerosis: focus on oxidized lipids and inflammation. Curr Opin Lipidol 12, 535-541
15. Martinet W and De Meyer GR (2009) Autophagy in atherosclerosis: a cell survival and death phenomenon with therapeutic potential. Circ Res 104, 304-317
16. Littlewood TD and Bennett MR (2003) Apoptotic cell death in atherosclerosis. Curr Opin Lipidol 14, 469-475
17. Kuhlencordt PJ, Gyurko R, Han F et al (2001) Accelerated atherosclerosis, aortic aneurysm formation, and ischemic heart disease in apolipoprotein E/endothelial nitric oxide synthase double-knockout mice. Circulation 104, 448-454
18. Strom A, Ahlqvist E, Franzen A, Heinegard D and Hultgardh-Nilsson A (2004) Extracellular

matrix components in atherosclerotic arteries of Apo E/LDL receptor deficient mice: an immunohistochemical study. Histol Histopathol 19, 337-347

19. Talusan P, Bedri S, Yang S et al (2005) Analysis of intimal proteoglycans in atherosclerosis-prone and atherosclerosis-resistant human arteries by mass spectrometry. Mol Cell Proteomics 4, 1350-1357
20. Cao L and Yang BB (1999) Chondrocyte apoptosis induced by aggrecan G1 domain as a result of decreased cell adhesion. Exp Cell Res 246, 527-537
21. Fujimoto T, Kawashima H, Tanaka T et al (2001) CD44 binds a chondroitin sulfate proteoglycan, aggrecan. Int Immunol 13, 359-366
22. Didangelos A, Mayr U, Monaco C and Mayr M (2012) Novel role of ADAMTS-5 protein in proteoglycan turnover and lipoprotein retention in atherosclerosis. J Biol Chem 287, 19341-19345
23. Stevens AL, Wheeler CA, Tannenbaum SR and Grodzinsky AJ (2008) Nitric oxide enhances aggrecan degradation by aggrecanase in response to TNF-alpha but not IL-1beta treatment at a post-transcriptional level in bovine cartilage explants. Osteoarthritis Cartilage 16, 489-497
24. Ross R, Glomset J, Kariya B and Harker L (1974) A platelet-dependent serum factor that stimulates the proliferation of arterial smooth muscle cells in vitro. Proc Natl Acad Sci U S A 71, 1207-1210
25. Gentleman RC, Carey VJ, Bates DM et al (2004) Bioconductor: open software development for computational biology and bioinformatics. Genome Biol 5, R80

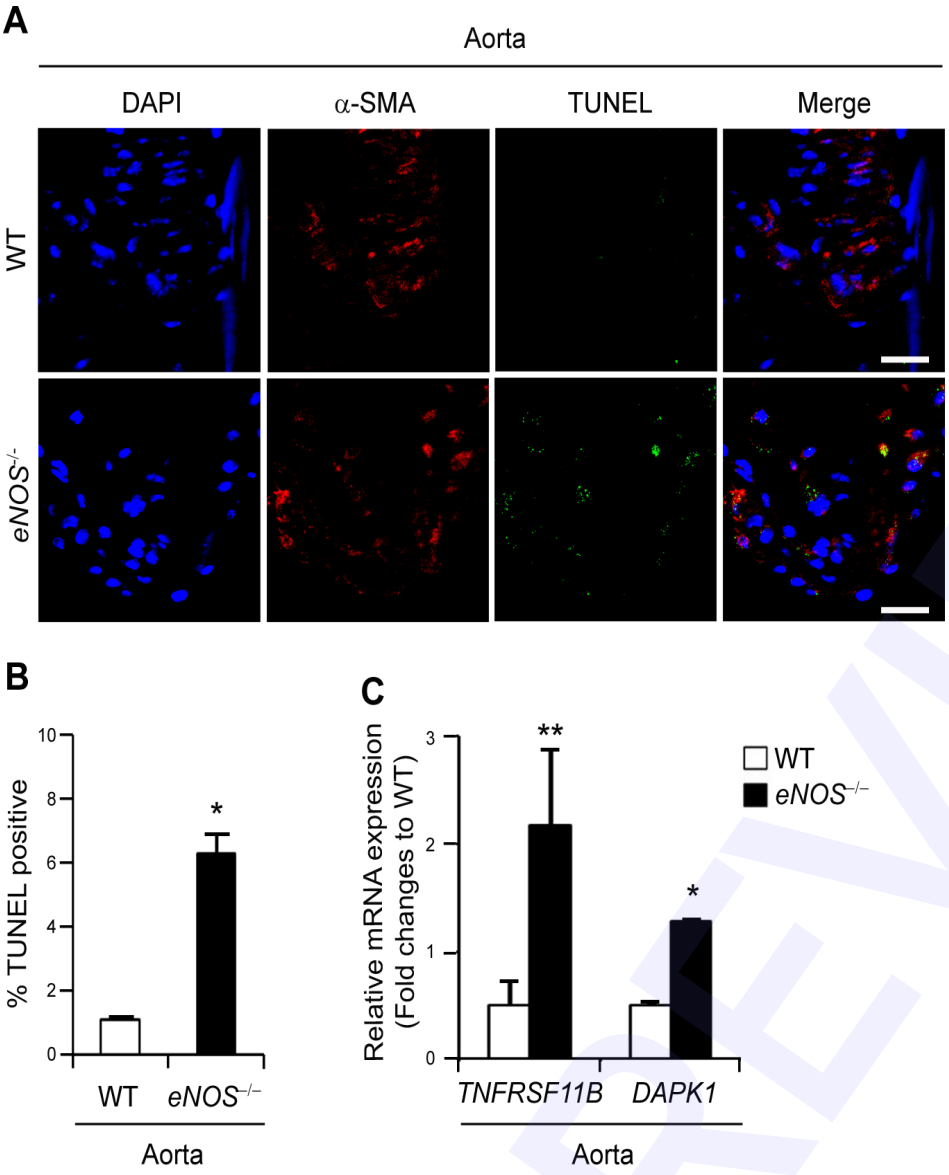

Figure 1

Fig. 1.

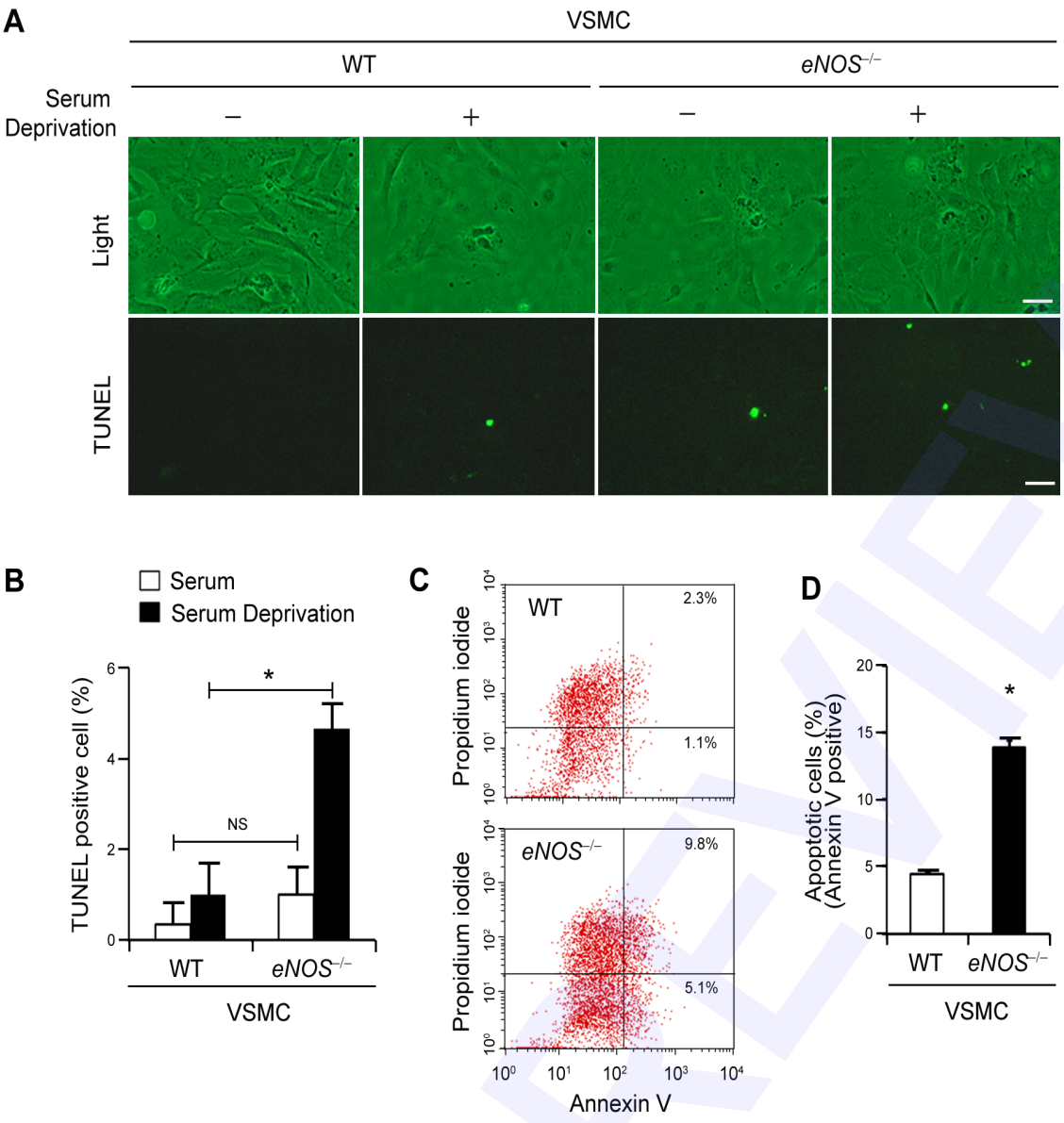

Figure 2

Fig. 2.

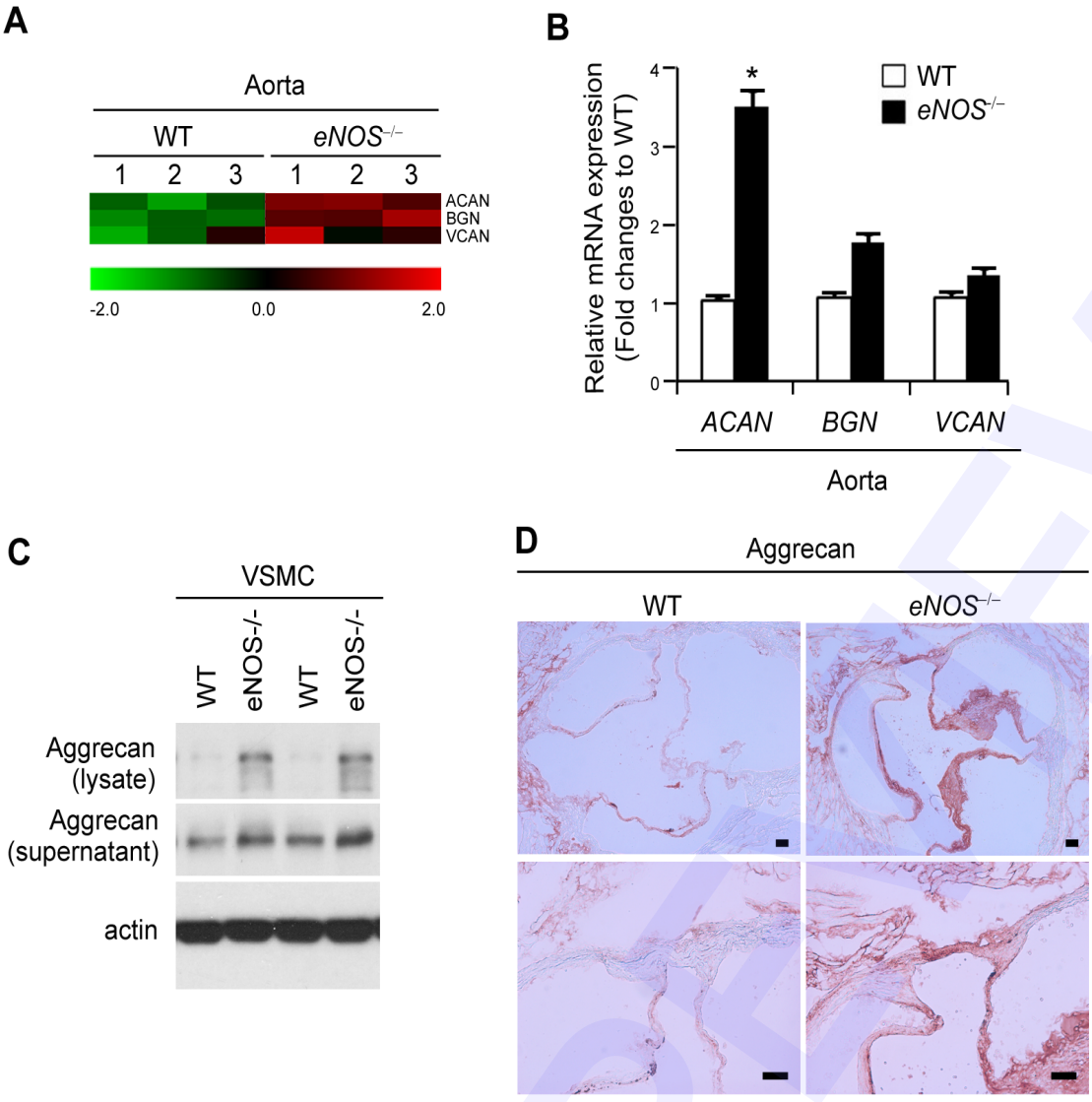

Figure 3

Fig. 3.

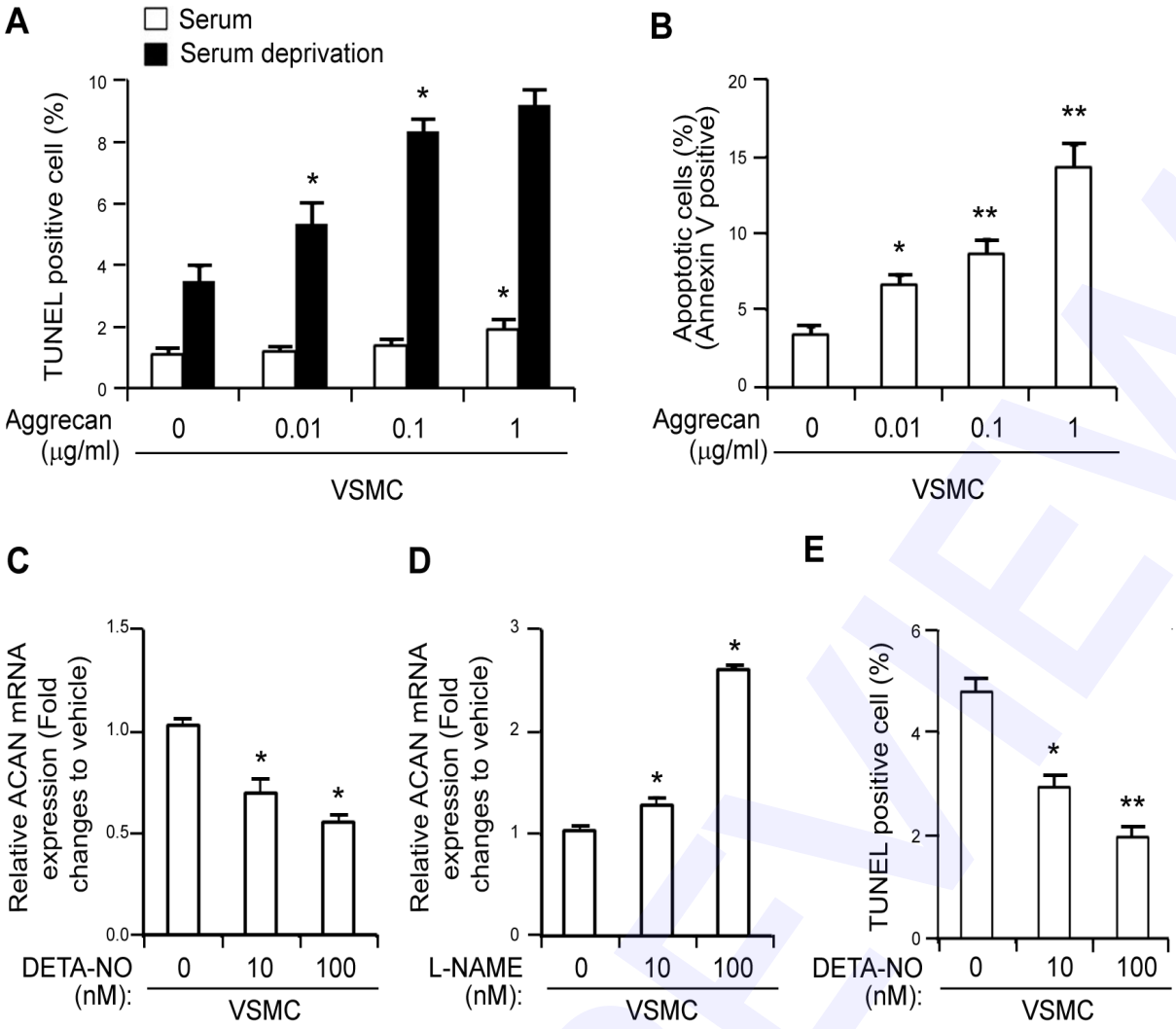

Figure 4

Fig. 4.

Supplementary Table 1. Genes upregulated in aortic tissue of *eNOS*$^{-/-}$

Functional Gene Grouping	Gene symbol	Full name	Biological function	†Fold changes
Atherosclerosis	*CTGF*	connective tissue growth factor	Adhesion, extracellular molecules, cell growth	+2.13
	FN1	fibronectin 1	Response to stress, adhesion, extracellular molecules	+1.91
	THBS4	thrombospondin 4	Adhesion, extracellular molecules	+1.98
Apoptosis	*TNFRSF11b*	tumor necrosis factor receptor superfamily, member 11b (osteoprotegerin)	DEATH domain proteins	+2.13
	DAPK1	death associated protein kinase 1	Induction of apoptosis, DEATH domain proteins	+1.70

†+: increase.